Talanta 105 (2013) 20–27

Contents lists available at SciVerse ScienceDirect

Talanta

journal homepage: www.elsevier.com/locate/talanta

Facile synthesis of Fe_3O_4@mesoporous TiO_2 microspheres for selective enrichment of phosphopeptides for phosphoproteomics analysis

Jin Lu, Mengyi Wang, Chunhui Deng *, Xiangmin Zhang

Department of Chemistry & Institutes of Biomedical Sciences, Fudan University, Shanghai 200433, China

ARTICLE INFO

Article history:
Received 18 August 2012
Received in revised form
9 November 2012
Accepted 10 November 2012
Available online 30 November 2012

Keywords:
Fe_3O_4@mesoporous TiO_2
Phosphopeptides
Selective enrichment
Mass spectrometry

ABSTRACT

Protein phosphorylation is one of the most important post-translational modifications. Due to the dynamic nature and low stoichiometry of the protein phosphorylation, enrichment of phosphopeptides from proteolytic mixtures is necessary prior to their characterization by mass spectrometry. In this work, we synthesized Fe_3O_4@mesoporous TiO_2 magnetic microspheres with core–shell structure and large surface area for selective enrichment of phosphopeptides. To demonstrate its ability for selective enrichment of phosphopeptides, we applied Fe_3O_4@mesoporous TiO_2 magnetic microspheres to isolation and enrichment of the phosphopeptides from tryptic digestion of standard proteins and real samples, and then the enriched peptides were analyzed by matrix-assisted laser desorption ionization mass spectrometry (MALDI-MS) or liquid chromatography coupled to electrospray ionization mass spectrometry (LC–ESI-MS). Due to that the as-made Fe_3O_4@mesoporous TiO_2 microspheres have large surface area, good dispersivity and biocompatibility, they have been demonstrated as a powerful tool for phosphoproteomics research.

1. Introduction

Post-translational modifications of proteins control many biological processes. The reversible phosphorylation of proteins is recognized as an essential post-translational modification regulating cell signaling and ultimately functions of biological systems. The significance of protein phosphorylation for a multitude of biological processes has resulted in major efforts to study protein phosphorylation for decades [1–3]. Unfortunately, due to the small quantity of phosphoproteins, the low stoichiometry of phosphorylation and the suppression effect by nonphosphorylated peptides, it remains a major challenge to detect them by mass spectrometry which is the most important and powerful tool for the analysis of protein phosphorylation [4–6].

A variety of approaches, including immunoprecipitation, chemical-modification strategies, strong cation exchange chromatography, immobilized metal affinity chromatography (IMAC) and metal oxide affinity chromatography (MOAC) have been used for this purpose [7–12]. Among these techniques, IMAC and MOAC are most simple and convenient and have been widely studied.

Titania has been investigated intensively in various areas including inorganic pigment, sunscreen, photocatalysis, energy storage, conversion, electrochromics, sensor fields and also proteomics [13–17]. Commendable specific interaction with phosphate group of phosphopeptides leads to their excellent enrichment efficiency of phosphopeptides [18–22]. The effectiveness of titania in practical applications varied considerably with its composition, crystallinity, morphology and texture of the material and specific surface area and mesoporosity [23–26]. Large specific surface area offers lots of interaction sites and then leads to good enrichment efficiency. Therefore, the controlled synthesis of titania materials with large specific surface area is badly in demand. Besides, magnetic materials have drawn a lot of attention in recent years because of their facility of separation and good biocompatibility [27–29]. Therefore synthesis of a magnetic titania material with large specific surface area is necessary.

In this work, we report the synthesis of monodisperse Fe_3O_4 @mesoporous TiO_2 with high specific surface area and application of them for the enrichment of phosphopeptides. They were evaluated with tryptic digests of both standard protein and a mouse brain lysate for the phosphoproteomics analysis. All the experimental results demonstrated a good enrichment efficiency and selectivity of the method we report here.

2. Materials and methods

2.1. Materials and chemicals

TFA was purchased from Merck (Darmstadt, Germany). ACN was HPLC grade from Fisher Scientific (Fairlawn, NJ, USA). Bovine β-casein, bovine serum albumin (BSA), ovalbumin (from chicken

* Corresponding author. Fax: +86 21 65641740.
E-mail address: chdeng@fudan.edu.cn (C. Deng).

0039-9140/$ - see front matter © 2012 Elsevier B.V. All rights reserved.
http://dx.doi.org/10.1016/j.talanta.2012.11.030

egg), trypsin (from bovine pancreas, TPCK treated), ammonium bicarbonate (NH_4HCO_3), dithiothreitol (DTT), iodoacetamide (IAA) 2, 5-dihydroxybenzoic acid (DHB) and phenylmethylsulfonyl fluoride (PMSF) were provided by Sigma-Aldrich Chemical (St. Louis, MO, USA). The water used in this study was purified using a Milli-Q water purification system from Millipore (Bedford, MA, USA).All other chemicals and reagents were of analytical grade and were purchased from Shanghai Chemical Reagent.

2.2. Characterization of Fe_3O_4@mesoporous TiO_2

The morphologies of the as-synthesized Fe_3O_4@mesoporous TiO_2 microspheres were studied under transmission electron microscopy (JEM-2100F) and scanning electron microscopy (XL30), respectively. Powder X-ray diffraction (XRD) patterns were recorded on a Bruker D4 X-ray diffractometer with Ni-filtered Cu K_R radiation (40 kV, 40 mA). Nitrogen adsorption and desorption isotherms were measured using Micromeritics ASAP 2020. The samples were degassed in a vacuum at 200 °C for 8 h prior to measurement. The Brunauer–Emmett–Teller (BET) method was utilized to calculate the specific surface areas (S_{BET}) using adsorption data in a relative pressure range from 0.18 to 0.35. By using the Barrett–Joyner–Halenda (BJH) model, the pore volumes and pore size distributions were derived from the desorption branches of the isotherms, and the total pore volumes (V_t) were estimated from the adsorbed amount at a relative pressure P/P_0 of 0.992.

2.3. Preparation of standard protein digests

Bovine β-casein, ovalbumin and Bovine serum albumin (BSA) were dissolved in 25 mM NH_4HCO_3 buffer at pH 8.3 and treated with trypsin (2%, w/w) for 16 h at 37 °C, respectively. Before the digestion, ovalbumin and BSA were reduced with DTT (final concentration 10 mM, 37 °C, 1 h) and carboxamidomethylated with iodoacetamide in the dark (final concentration 20 mM, 37 °C, 30 min). Bovine β-casein was digested directly.

2.4. Preparation of the lysate of mouse brain

Mouse brain extract was enriched and analyzed by nano LC–MS/MS. Mice were firstly dissected, and the brain was promptly disemboweled and washed with cold physiological saline to remove the blood and some possible contaminant. The tissue specimens was placed in ice-cold homogenization buffer consisting of 7 M urea, 2 M thiourea and a mixture of protease inhibitor (1 mM phenylmethanesulphonylfluoride) and phosphatase inhibitors (0.2 mM Na_3VO_4, 1 mM NaF). After mincing with scissors and washing to remove blood, the brains were homogenized in a Pottter–Elvejhem homogenizer with a Teflon piston, using 5 mL of the homogenization buffer per 1 g of tissue. The suspension was homogenized for approximately 2 min, vortexed at 0 °C for 30 min, and centrifuged at 22,000*g* for 1.5 h. The supernatant contained the total brain proteins.

Appropriate volumes of protein sample were precipitated as above, lyophilized to dryness, and redissolved in reducing solution (6 M guanidine hydrochloride, 100 mM NH_4HCO_3, pH=8.3) with the protein concentration adjusted to 2 μg/μL. Then, 200 μg of this protein sample (100 μL volume) were mixed with 10 μL of 0.5 M DTT. The mixture was incubated at 37 °C for 1 h, and then 20 μL of 0.5 M 2-iodoacetamide were added and incubated for an additional 30 min at 37 °C in the dark. The protein mixtures were exchanged into 50 mM NH_4HCO_3 buffer, pH=8.5, and incubated with trypsin (50:1) at 37 °C overnight.

2.5. Selectively enrichment of phosphopeptides from tryptic digestion of standard proteins and mouse brain

For the standard proteins, first, the peptide mixtures originating from tryptic digestions were diluted by 50% acetonitrile and 0.1% TFA aqueous solution (v/v), and suspension of Fe_3O_4@mesoporous TiO_2 microspheres (400 μg) was added into 200 μL of diluted peptide mixture. Then the mixed solutions were vibrated at 25 °C for 30 min. After that, with the help of magnet, the pellucid solutions were taken out. After that, the Fe_3O_4@mesoporous TiO_2 microspheres were washed with 50% acetonitrile and 0.1% TFA aqueous solution (v/v) for three times. Finally the peptides captured by Fe_3O_4@mesoporous TiO_2 microspheres were

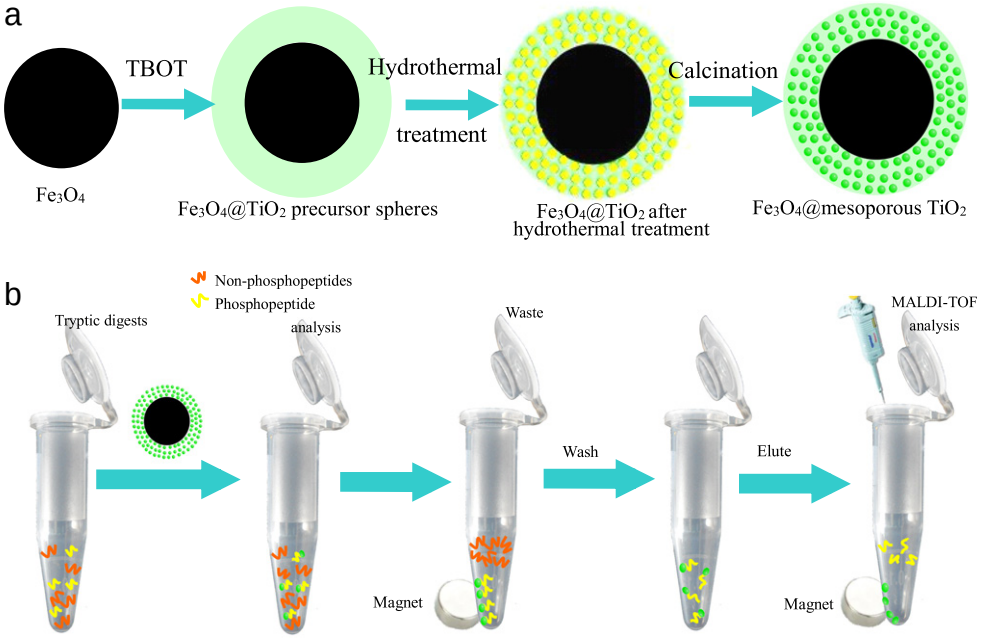

Scheme 1. (a) Schematic diagram of the synthetic route of Fe_3O_4@mesoporous TiO_2, (b) enrichment protocol for phosphopeptides by using Fe_3O_4@mesoporous TiO_2.

eluted with 5 μL of 0.4 M ammonia aqueous solution for 10 min and the eluate was analyzed by MALDI-TOF MS.

The tryptic digests of mouse brain were lyophilized and then dissolved in loading buffer. Two microgram of Fe_3O_4@mesoporous TiO_2 microspheres were added into 400 μL of diluted mouse brain digests. Then the mixed solutions were vibrated at 25 °C for 30 min. After that, with the help of magnet, the phosphopeptides adsorbed to Fe_3O_4@mesoporous TiO_2 microspheres were collected and washed with 50% (v/v) acetonitrile and 0.1% (v/v) TFA aqueous solution for three times. Then the Fe_3O_4@mesoporous TiO_2 microspheres were eluted with 50 μL of 0.4 M ammonia aqueous solution for 30 min.The eluate was lyophilized and then dissolved in 35 μL loading phase. Finally, the solution was submitted for LC–ESI-MS analysis.

2.6. Mass spectrometry and database searching

2.6.1. MALDI-TOF MS analysis

For MALDI-TOF MS, sample solutions (0.5 μL) were deposited on plate using the dried droplet method, and then another 0.5 μL of DHB matrix solution (20 mg/mL, in 50% acetonitrile and 1% H_3PO_4 aqueous solution (v/v)) was introduced as a matrix. Analysis of peptides was performed by MALDI-TOF MS on a 5800 Proteomics Analyzer (Applied Biosystems) in the reflector TOF detection modes. The sample was excited using an Nd:YAG laser (383 nm) operated at a repetition rate of 200 Hz and acceleration voltage of 20 kV. All spectra were taken from signal-averaging of 800 laser shots with the laser intensity kept at a proper constant.

2.6.2. Nano-LC–ESI-MS/MS analysis

The peptide solution eluted from microspheres were dried thoroughly by lyophilization and then redissolved with 5% ACN aqueous solution containing 0.1% formic acid, separated by nano-LC and analyzed by on-line electrospray tandem mass spectrometry. The experiments were performed on a Nano Aquity UPLC system (Waters Corporation, Milford, USA) connected to an LTQ Orbitrap XL mass spectrometer (Thermo Electron Corp., Bremen, Germany) equipped with an online nanoelectrospray ion source (Michrom Bioresources, Auburn, USA). The separation of the peptides was performed in a Symmetry® C18, 5 μm, 180 μm id × 2 cm trap-column and a BEH300 C18, 1.7 μm, 75 μm id × 15 cm reverse phase column (Waters Corporation, Milford, USA).

The peptide dissolution were injected onto the trap-column with a flow of 15 μL min^{-1} for 3 min and subsequently eluted with a three-step linear gradient. Starting from 5% B to 45% B in 43 min (mobile phase A: 5% ACN aqueous solution with 0.1% formic acid; mobile phase B: 95% ACN aqueous solution with 0.1% formic acid), increased to 80% B in 3 min. After holding on 80% B for 1 min, it decreased to the initial condition of 5% B in 1 min. Finally, the column was re-equilibrated at 5% B for 12 min. The column flow rate was maintained at 300 nL/min and column temperature was maintained at 35 °C. The electrospray voltage of 1.4 kV versus the inlet of the mass spectrometer was used. LTQ Orbitrap XL mass spectrometer was operated in the data-dependent mode to switch automatically between MS and MS/MS acquisition. Survey full-scan MS spectra with two microscans (m/z 400–1800) were acquired in the Orbitrap with a mass resolution of 60,000 at m/z 400, followed by ten sequential LTQ-MS/MS scans. Dynamic exclusion was used with two repeat counts, 10-s repeat duration, and 60-s exclusion duration. For MS/MS, precursor ions were activated using 25% normalized collision energy at the default activation q of 0.25.

The obtained LTQ Orbitrap XL MS/MS data were identified by using SEQUEST [v.28 (revision 12)], Thermo Electron Corp. against the mouse International Protein Index (IPI) database. To reduce false positive identification results, a decoy database containing the reverse sequences was introduced into the database. The searching parameters were set up as follows: enzyme; the variable modification was phosphorylation (S, T, Y) and oxidation of methionine; the peptide mass tolerance was 100 ppm, and the MS/MS tolerance was 1 Da. And then the obtained searching results were filtrated with following parameters: $\Delta Cn > 0.1$; the minimum Xcorr of 2.00, and 2.50 corresponding to 2+, and 3+ charge states, respectively. Based on the above parameters, false positive rate of less than 5% was

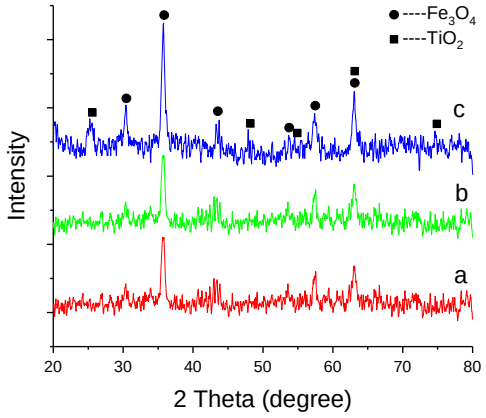

Fig. 2. Wide-angle XRD patterns of (a) Fe_3O_4@TiO_2 precursor spheres (b) Fe_3O_4@TiO_2 after hydrothermal treatment (c) Fe_3O_4@mesoporous TiO_2.

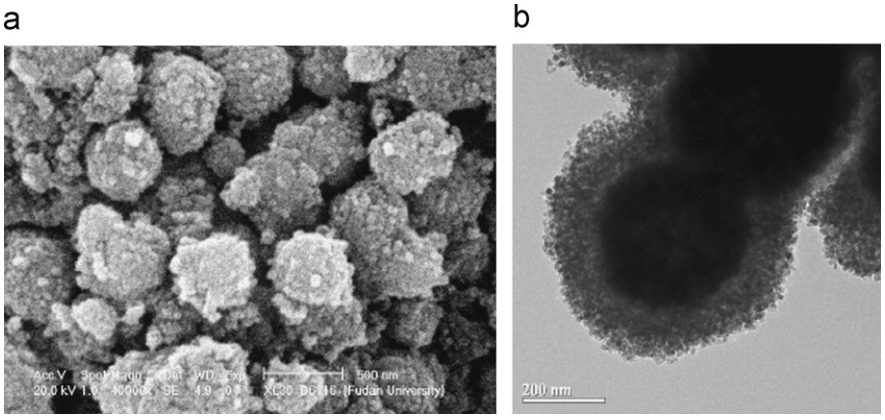

Fig. 1. (a) SEM of Fe_3O_4@mesoporous TiO_2 (b) TEM of Fe_3O_4@mesoporous TiO_2.

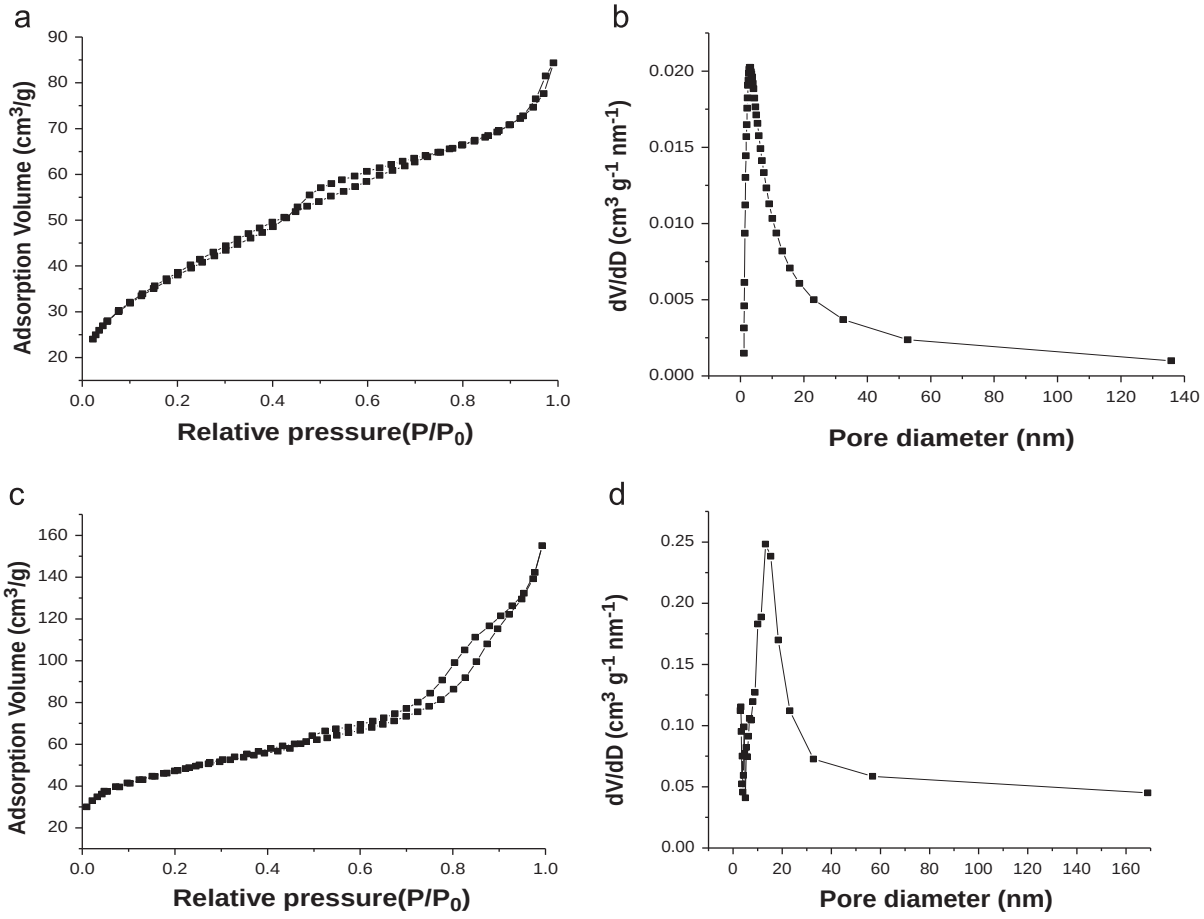

Fig. 3. N_2 adsorption–desorption isotherms of (a) Fe_3O_4@TiO_2 precursor spheres (c) Fe_3O_4@mesoporous TiO_2 and pore size distribution of (b) Fe_3O_4@TiO_2 precursor spheres (d) Fe_3O_4@mesoporous TiO_2.

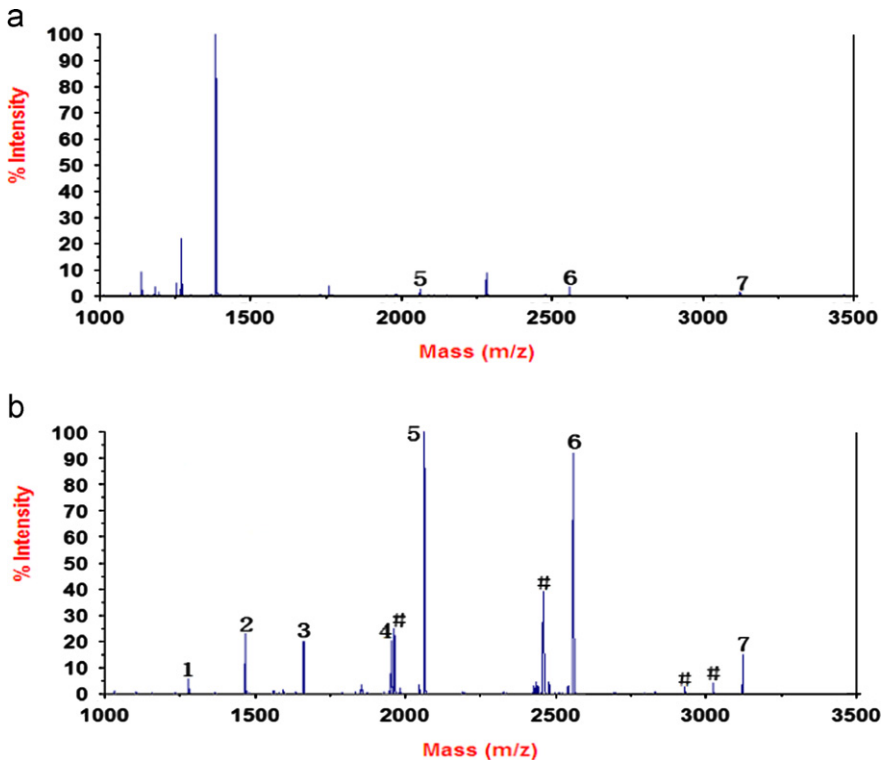

Fig. 4. MALDI-TOF mass spectra of peptides derived from β-casein: (a) without enrichment (b) enriched by Fe_3O_4@mesoporous TiO_2. Phosphopeptide ions identified are marked with numbers. # the metastable losses of phosphoric acid.

calculated to remove low-probability peptides, demonstrating the reliability of the identified results in this investigation.

3. Results and discussion

3.1. Synthesis and characterization of Fe_3O_4@mesoporous TiO_2 microspheres

The designed synthesis strategy of Fe_3O_4@mesoporous TiO_2 microspheres is shown in Scheme 1. First, magnetic Fe_3O_4 microspheres were synthesized using our previous reported method, then Fe_3O_4@TiO_2 precursor spheres were synthesized based on the hydrolysis and condensation of TBOT. The above obtained Fe_3O_4 microspheres (0.15 g) were redispersed in absolute ethanol (200 mL), and mixed with concentrated ammonia solution (0.9 mL, 28 wt%) under ultrasound for 15 min. Afterward, 2.0 mL of TBOT was added dropwise in 5 min, and the reaction was allowed to proceed for 24 h at 45 °C under continuous mechanical stirring. After washing with deionized water and ethanol for 3 times, the above obtained Fe_3O_4@TiO_2 precursor spheres (0.5 g) were mixed with 20 mL deionized water, then added into a Teflon-lined stainless-steel autoclave (30 mL in capacity). The autoclave was heated at 160 °C for 24 h, and then allowed to cool to room temperature. The resultant product was separated and collected with a magnet, followed by washing with deionized water and ethanol for 3 times, respectively. At last the product was dried under vacuum at 50 °C and calcined in nitrogen at 400 °C for 2 h. After the furnace was left to cool to room temperature, the final products were transferred to tubes and preserved under room temperature.

The morphology of prepared microspheres was obtained by scanning electron microscopy (SEM) and transmission electron microscopy (TEM). Fe_3O_4@TiO_2 precursor spheres are monodispersed and have nearly uniform size (Fig. S1a). An obvious

Table 1
Detail information of the observed phosphopeptides obtained from tryptic digestion of α-casein S1 and S2, and β-casein[a].

Peak number	Theoretical *m/z*	Observed *m/z*	aa	Peptide sequence
1	1278.6	1278.9	β/33–52	FQSEEQQQTEDELQDKIHPF
2	1466.6	1466.7	α-S2/153–164	TVDMSTEVFTK
3	1660.8	1660.9	α-S1/106–119	VPQLEIVPNSAEER
4	1952.0	1952.1	α-S1/104–119	YKVPQLEIVPNSAEER
5	2061.8	2061.8	β/33–48	FQSEEQQQTEDELQDK
6	2556.1	2556.2	β/33–52	FQSEEQQQTEDELQDKIHPF
7	3122.3	3122.3	β/1–25	RELEELNVPGEIVESLSSSEESITR

[a] The phosphorylation sites are underlined.

Table 2
Detail information of the observed phosphopeptides obtained from tryptic digestion of ovalbumin[a].

Theoretical *m/z*	Observed *m/z*	aa	Peptide sequence
2088.9	2089.0	Ova/340–359	EVVGSAEAGVDAASVSEEFR

[a] The phosphorylation sites are underlined.

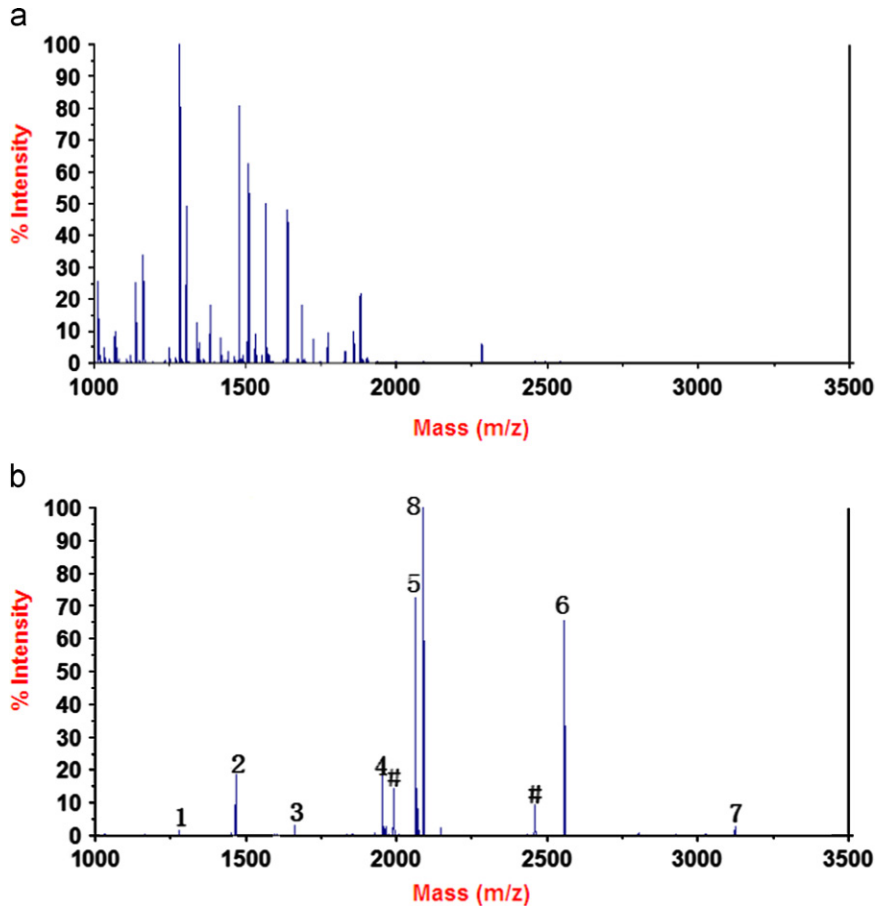

Fig. 5. MALDI-TOF mass spectra of peptides derived from a peptide mixture of β-casein, ovalbumin and BSA at a molar ratio of 1:1:50: (a) without enrichment (b) enriched by Fe_3O_4@mesoporous TiO_2.

mesoporous TiO_2 shell (~37 nm) was observed and the mean diameter of the precursor spheres is about 220 nm (Fig. S1b). As shown in Fig. 1a, after solvothermal and calcination treatments of these precursor spheres the monodispersity of the spheres were retained. It is worth nothing that after solvothermal and calcination treatments, amorphous dense TiO_2 transformed to a large number of crystallization TiO_2 nanoparticles (Fig. 1b); this was confirmed with the corresponding Wide-angle X-ray diffraction pattern (Fig. 2).

The energy-dispersive X-ray analysis (EDXA) (Fig. S2) of the illuminating electron beams on the obtained Fe_3O_4@mesoporous TiO_2 reveals the existence of Fe, Ti, Cu and O elements (the Cu peaks in the spectrum originate from the Cu TEM grid), further confirming the successful coating of TiO_2.

Wide-angle X-ray diffraction patterns of the Fe_3O_4@TiO_2 precursor spheres, Fe_3O_4@TiO_2 after hydrothermal treatment and Fe_3O_4@mesoporous TiO_2 are shown in Fig.2. Before calcination, TiO_2 nanoparticles are amorphous (Fig. 2a and b) and after calcination treatment Fe_3O_4@mesoporous TiO_2 show well-resolved diffractions peaks which are well-matched to Fe_3O_4 (JCPDS 65-3107) and anatase (JCPDS 21-1272) (Fig. 2c), suggesting that their frameworks are crystalline and our obtained products are Fe_3O_4@mesoporous TiO_2.

Additionally, the porosity of the microspheres before and after the subsequent solvothermal and calcination treatments was characterized by nitrogen sorption at 77 K. Fig. 3a and b display the N_2 adsorption–desorption isotherm and the corresponding pore size distribution curve for the Fe_3O_4@TiO_2 precursor spheres, while Fig. 3c and d display that of Fe_3O_4@mesoporous TiO_2. The BET surface area and total pore volume of Fe_3O_4@TiO_2 precursor spheres were calculated to be 139.8 $m^2\,g^{-1}$ and 0.13 $cm^3\,g^{-1}$, respectively, and the results of Fe_3O_4@mesoporous TiO_2 were calculated to be 162.6 $m^2\,g^{-1}$ and 0.24 $cm^3\,g^{-1}$, respectively. That indicate that the sample has a relatively high surface-to-volume

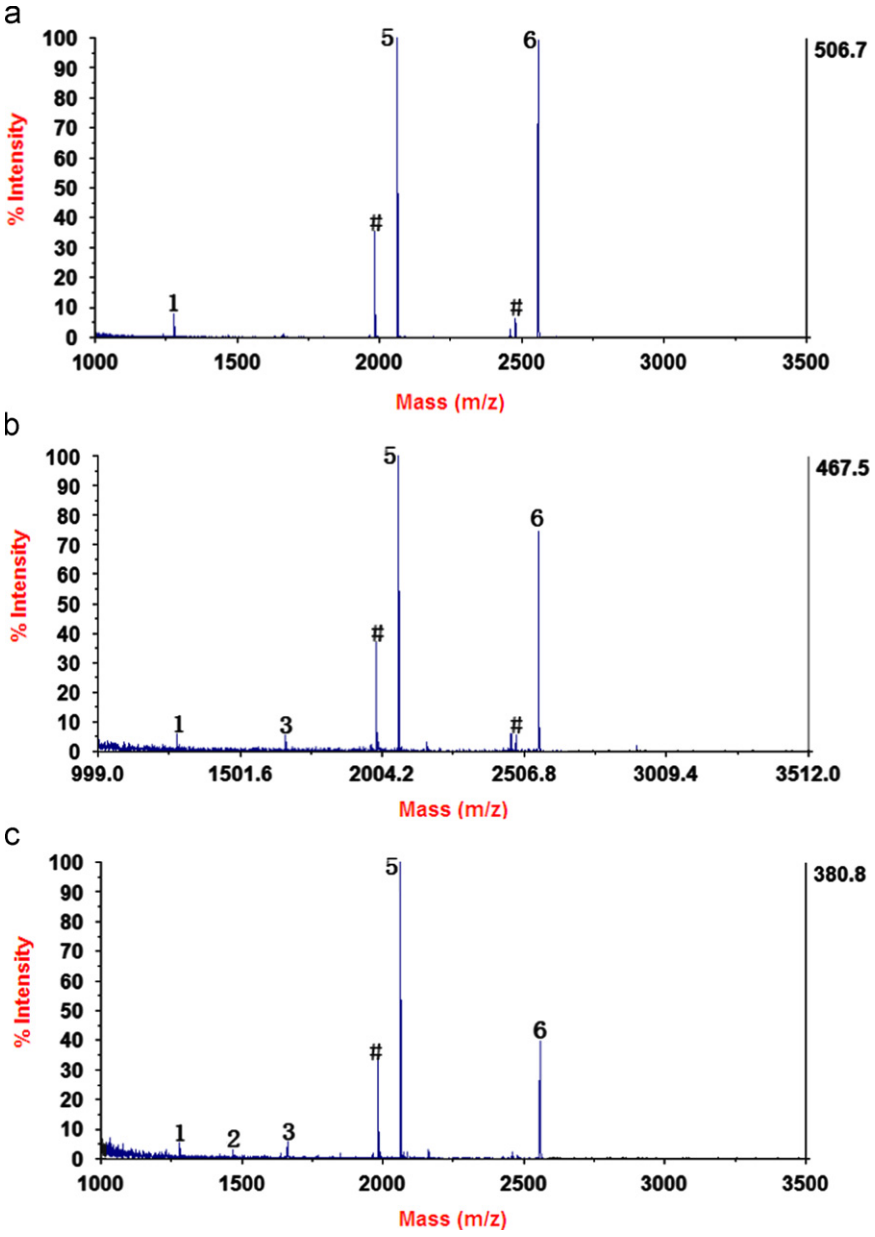

Fig. 6. MALDI-TOF mass spectra of phosphopeptides enriched from β-casein with different concentrations: (a) 4×10^{-9} M (b) 2×10^{-9} M (c) 4×10^{-10} M using Fe_3O_4@mesoporous TiO_2. Phosphopeptide ions identified are marked with numbers. # the metastable losses of phosphoric acid.

ratio and after solvothermal and calcination treatments, the specific surface area gets larger, confirming the solvothermal and calcination treatments are necessary to attain a higher surface area [30,31].

3.2. Selective enrichment of phosphopeptides from tryptic digestion of standard proteins

The Fe_3O_4@mesoporous TiO_2 were first used to isolate phosphopeptides from tryptic digests of β-casein, which is commonly contaminated with a trace of α-casein. A direct analysis of 4×10^{-7} M β-casein by MALDI-TOF MS indicates that signals of phosphopeptides were feeble and the nonphosphorylated peptides dominate the spectrum (Fig. 4a). However, after enrichment by Fe_3O_4@mesoporous TiO_2, the signals for the β-casein phosphopeptides (marked with numbers) significantly increase and dominate the spectrum (Fig. 4b). Furthermore, three phosphopeptides derived from α-casein were also observed and nearly no nonphosphorylated peptides were observed, indicating a high enrichment efficiency of the Fe_3O_4@mesoporous TiO_2. The signals marked with a circumflex could be assigned to a dephosphorylated fragment of phosphopeptide through loss of H_3PO_4. The observed phosphopeptides are marked with numbers and the detailed information of the observed phosphopeptides is listed in Table 1.

To evaluate the specificity of enrichment of phosphopeptides with Fe_3O_4@mesoporous TiO_2, a relatively complex sample consisting of a peptide mixture originating from a tryptic digest of β-casein (4×10^{-8} M), ovalbumin (4×10^{-8} M) and bovine serum albumin (2×10^{-6} M) with a ratio of 1:1:50, was used as the test sample. The spectrum obtained for MALDI-TOF MS of the peptide mixture is shown in Fig. 5a. The MS spectrum for the analysis of phosphopeptides enriched with Fe_3O_4@mesoporous TiO_2 is shown in Fig. 5b. It is obvious that nearly no nonphosphopeptides were described in Fig. 5b and we can see that besides the spectrum of α-casein and β-casein, we successfully enriched one phosphopeptide of ovalbumin at 2089.0 *m/z*. The detailed information of the observed phosphopeptide of ovalbumin was listed in Table 2. This suggests that Fe_3O_4 @mesoporous TiO_2 could specifically isolate and enrich the phosphopeptides.

To study the detection limit of the Fe_3O_4@mesoporous TiO_2 used for enrichment of phosphopeptides, β-casein digest solutions with different concentrations were applied. The mass spectra are shown in Fig. 6. It can be seen that when the concentration of β-casein digest is 4×10^{-10} M, after enrichment by the Fe_3O_4@mesoporous TiO_2, the ion signals from the phosphopeptides is still powerful, which indicates the high detection sensitivity of the microspheres [32–34]. The results suggest that the Fe_3O_4@mesoporous TiO_2 we report here are promising materials for the enrichment of phosphopeptides.

3.3. Selective enrichment of phosphopeptides from tryptic digestion of rat brain

To further evaluate the performance of Fe_3O_4@mesoporous TiO_2 for phosphopeptide enrichment, the microspheres were employed to enrich phosphopeptides from tryptic digest of mouse brain. After database searching, information of the enriched phosphopeptide was obtained. In total, 1774 phosphorylation sites of 731 phosphopeptides-1082 on serine (60.99%), 510 on threonine (28.75%) and 182 on tyrosine (10.26%)—were identified. The detailed information of the phosphopeptides enriched from tryptic digests of mouse brain by using Fe_3O_4@mesoporous TiO_2 are listed in the ESI (see Table S1).

4. Conclusions

In summary, we successfully synthesized Fe_3O_4@mesoporous TiO_2 with well-defined core shell structure and large specific surface area, and demonstrated their potential for efficient and selective enrichment of phosphopeptides. In the study, Fe_3O_4@-mesoporous TiO_2 were demonstrated to have the ability for selective enrichment of phosphopeptides by using standard protein digestion. Furthermore, we applied Fe_3O_4@mesoporous TiO_2 for selective enrichment of phosphopeptides from tryptic digestion of mouse brain, and the experimental results showed that the approach based on Fe_3O_4@mesoporous TiO_2 would be effective for phosphopeptides enrichment.

Acknowledgements

This work was supported by the National Basic Research Priorities Program (2012CB910601, 2013CB911201), the National Natural Science Foundation of China (21075022, 21275033, 21105016), Graduate Innovation Fund of Fudan University, Research Fund for the Doctoral Program of Higher Education of China (20110071110007 and 20100071120053), Shanghai Municipal Natural Science Foundation (11ZR1403200) and Shanghai Leading Academic Discipline Project (B109).

Appendix A. Supporting information

Supplementary data associated with this article can be found in the online version at http://dx.doi.org/10.1016/j.talanta.2012.11.030.

References

[1] T. Hunter, Philos. Trans. R. Soc. Lond. B: Biol. Sci. 353 (1998) 583–605.
[2] D.E. Kalume, H. Molina, A. Pandey, Curr. Opin. Chem. Biol. 7 (2003) 64–69.
[3] J.D. Graves, E.G. Krebs, Pharmacol. Ther. 82 (1999) 111–121.
[4] M.O. Collins, L. Yu, J.S. Choudhary, Proteomics 7 (2007) 2751–2768.
[5] O.N. Jensen, Nat. Rev. Mol. Cell Biol. 7 (2006) 391–403.
[6] E.S. Witze, W.M. Old, K.A. Resing, N.G. Ahn, Nat. Methods 4 (2007) 798–806.
[7] A. Gruhler, J.V. Olsen, S. Mohammed, P. Mortensen, Mol. Cell. Proteomics 4 (2005) 310–327.
[8] Y. Li, D.W. Qi, C.H. Deng, P.Y. Yang, X.M. Zhang, J. Proteome Res. 7 (2008) 1767–1777.
[9] Y. Oda, T. Nagasu, B.T. Chait, Nat. Biotechnol. 19 (2001) 379–382.
[10] M.R. Larsen, T.E. Thingholm, O.N. Jensen, Mol. Cell. Proteomics 4 (2005) 873–886.
[11] D.W. Qi, Y. Mao, J. Lu, C.H. Deng, X.M. Zhang, J. Chromatogr. A 1217 (2010) 2606–2617.
[12] C.T. Chen, Y.C. Chen, Chem. Commun. 46 (2010) 5674–5676.
[13] A. Fujishima, X.T. Zhang, D.A. Tryk, Surf. Sci. Rep. 63 (2008) 515–582.
[14] M. Gratzel, Nature 414 (2001) 338–344.
[15] J. Wijnhoven, W.L. Vos, Science 281 (1998) 802–804.
[16] A. Heller, Acc. Chem. Res. 28 (1995) 503–508.
[17] T.A. Gad-Allah, K. Fujimura, S. Kato, S. Satokawa, T. Kojima, J. Hazard. Mater. 154 (2008) 572–577.
[18] M.W.H. Pinkse, P.M. Uitto, M.J. Hilhorst, B. Ooms, A.J.R. Heck, Anal. Chem. 76 (2004) 3935–3943.
[19] Y. Li, J.S. Wu, D.W. Qi, X.Q. Xu, C.H. Deng, P.Y. Yang, X.M. Zhang, Chem. Commun. 162 (2008) 564–566.
[20] J. Lu, M.Y. Wang, Y. Li, C.H. Deng, Nanoscale 4 (2012) 1577–1580.
[21] A. Montoya, L. Beltran, P. Casado, J.C. Rodriguez-Prados, P.R. Cutillas, Methods 54 (2011) 370–378.
[22] W.F. Ma, Y. Zhang, L.L. Li, L.J. You, P. Zhang, Y.T. Zhang, J.M. Li, M. Yu, J. Guo, H.J. Lu, C.C. Wang, ACS Nano 6 (2012) 3179–3188.
[23] D.I. Enache, J.K. Edwards, P. Landon, B. Solsona-Espriu, A.F. Carley, A.A. Herzing, M. Watanabe, C.J. Kiely, D.W. Knight, G.J. Hutchings, Science 311 (2006) 362–365.
[24] B.Z. Tian, X.Y. Liu, B. Tu, C.Z. Yu, J. Fan, L.M. Wang, S.H. Xie, G.D. Stucky, D.Y. Zhao, Nat. Mater. 2 (2003) 159–163.
[25] X.H. Wang, J.G. Li, H. Kamiyama, M. Katada, N. Ohashi, Y. Moriyoshi, T. Ishigaki, J. Am. Chem. Soc. 127 (2005) 10987 10982.
[26] J. Lee, M.C. Orilall, S.C. Warren, M. Kamperman, F.J. Disalvo, U. Wiesner, Nat. Mater. 7 (2008) 222–228.

[27] H.M. Chen, X.Q. Xu, N. Yao, C.H. Deng, P.Y. Yang, X.M. Zhang, Proteomics 8 (2008) 2778–2784.
[28] H.M. Chen, D.W. Qi, C.H. Deng, P.Y. Yang, X.M. Zhang, Proteomics 9 (2009) 380–387.
[29] J. Lu, Y. Li, C.H. Deng, Nanoscale 3 (2011) 1225–1233.
[30] D.H. Chen, L. Cao, F.Z. Huang, P. Imperia, Y.B. Cheng, R.A. Caruso, J. Am. Chem. Soc. 132 (2010) 4438–4444.
[31] W. Li, Y.H. Deng, Z.X. Wu, X.F. Qian, J.P. Yang, W. Yao, D. Gu, F. Zhang, B. Tu, D.Y. Zhao, J. Am. Chem. Soc. 133 (2011) 15830–15833.
[32] J. Lu, Y. Li, C.H. Deng, Nanoscale 3 (2011) 1225–1233.
[33] D.W. Qi, J. Lu, C.H. Deng, X.M. Zhang, J. Phys. Chem. C. 113 (2009) 15854–15861.
[34] N. Zhang, H.Y. Peng, B. Hu, Talanta 94 (2012) 278–283.